Quantum dark solitons in the one-dimensional Bose gas

Sophie S. Shamailov and Joachim Brand

Phys. Rev. A **99**, 043632 — Published 30 April 2019

DOI: 10.1103/PhysRevA.99.043632

Quantum dark solitons in the one-dimensional Bose gas

Sophie S. Shamailov* and Joachim Brand†
Dodd-Walls Centre for Photonics and Quantum Technology, New Zealand and
New Zealand Institute for Advanced Study, Centre for Theoretical Chemistry and Physics,
Massey University, Private Bag 102904, North Shore, Auckland 0745, New Zealand
(Dated: April 4, 2019)

Dark and grey soliton-like states are shown to emerge from numerically constructed superpositions of translationally-invariant eigenstates of the interacting Bose gas in a toroidal trap. The exact quantum many-body dynamics reveals a density depression with ballistic spreading that is absent in classical solitons. A simple theory based on finite-size bound states of holes with quantum-mechanical center-of-mass motion quantitatively explains the time-evolution and predicts quantum effects that could be observed in ultra-cold gas experiments. The soliton phase step is found relevant for explaining finite size effects in numerical simulations. An invariant fundamental soliton width is shown to deviate from the Gross-Pitaevskii predictions in the interacting regime and vanishes in the Tonks-Girardeau limit.

I. INTRODUCTION

Dark solitons [1] are ubiquitous features of superfluids and have been observed frequently in ultra-cold atomic gas experiments [2–9]. The characteristic localised density depression is stabilised by the competing effects of hydrostatic pressure and the stiffness of the superfluid phase. While experiments to date could be well explained by classical theory, there has been much debate about quantum effects [9–12]. Quantum features of dark solitons are expected to be particularly relevant under reduced dimensionality, where quantum fluctuations destroy long-range coherence of the superfluid phase. While theoretical works on the one-dimensional Bose gas have predicted effects like greying of the dark soliton [11–15], and have pointed to a connection of dark solitons to quantum-many-body eigenstates of the Bethe-ansatz solvable Lieb-Liniger model [10, 16–24], the full picture connecting the physical effects with the exact eigenstates is still missing.

Specifically, Ref. [17] showed that the dispersion relation of yrast states (eigenstates with lowest energy at given momentum) in the Lieb-Liniger model asymptotically approaches that of dark solitons in the Gross-Pitaveskii (GP) or classical nonlinear Schrödinger equation in the high-density limit. However, in contrast to the translationally-invariant yrast states of constant particle density, classical dark solitons have a localised density dip that propagates with constant velocity. On the other hand, numerical simulations of single-shot measurements of particle position in the yrast states show localised voids appearing at random positions [22, 25]. Superpositions of yrast states were further shown to exhibit translational symmetry breaking under weak interactions [19, 20], and localised density depressions at finite interactions that decay during time evolution [23, 24]. However, control over soliton parameters, the classical limit, or quantitative understanding of beyond mean-field effects were not achieved.

The situation is better understood for bright solitons, where quantum effects were observed in optics experiments [26, 27] and a full quantum theory was developed by constructing quantum soliton states as superpositions of translationally invariant eigenstates of an interacting boson model [28–31].

In this work we bridge the gap in the quantum theory of dark solitons by constructing quantum many-body states that most-closely resemble classical dark solitons from superpositions of yrast eigenstates, and quantifying their properties. We simulate the full quantum dynamics making use of exact solutions from the Bethe ansatz. While the behavior of classical dark solitons is recovered in the high density limit, we observe ballistic spreading in the crossover to the low-density, strongly-correlated limit, known as the Tonks-Girardeau gas. Modeling the quantum dark soliton as a finite-size quantum mechanical quasiparticle (inspired by Ref. [32]), we identify the velocity, a soliton mass, and a fundamental soliton width as characteristic parameters for the dynamics of the simulated density depletion. These parameters can be obtained from the yrast dispersion relation with finite size corrections, attaining excellent agreement with the numerical simulations. The particle number depletion and a quantity interpreted as the soliton phase step play important roles in the finite size corrections and can also be computed from the dispersion relation.

II. YRAST STATES IN THE LIEB-LINIGER MODEL

We model a gas of N bosonic atoms with mass m in a tightly-confining toroidal trap of circumference L by the Lieb-Liniger model [33, 34] with repulsive interactions $c > 0$ [35]

$$\hat{H} = -\frac{\hbar^2}{2m}\sum_{i=1}^{N}\frac{\partial^2}{\partial x_i^2} + \frac{\hbar^2 c}{m}\sum_{i<j}\delta(x_i - x_j). \qquad (1)$$

The eigenstates of H can be constructed with the Bethe ansatz from the set of N rapidities $\{k_j\}$, which in turn is fully determined by N quantum numbers I_j through the Bethe equations

$$k_j + \frac{1}{L}\sum_l 2\arctan\frac{k_j - k_l}{c} = \frac{2\pi}{L}I_j, \qquad (2)$$

where the $I_j(+\frac{1}{2})$ take integer values for odd (even) N [36]. While the momentum $P = \hbar\sum_j k_j = 2\pi\hbar/L\sum_j I_j$ is al-

* s.shamailov@auckland.ac.nz; Present address: Dodd-Walls Centre for Photonics and Quantum Technology, Department of Physics, University of Auckland, Private Bag 92019, Auckland, New Zealand
† j.brand@massey.ac.nz

ready determined by the quantum numbers I_j, the energy $E = \hbar^2/2m\sum_j k_j^2$ depends on the interaction strength through the rapidities. Of particular relevance are *yrast* states denoted by $|P, \mathrm{yr}\rangle$, which are the eigenstates of lowest energy E_P^N for given P and N. They are found from otherwise contiguous sets of I_j with a gap of up to one quantum number.

III. QUANTUM DARK SOLITONS

We construct initial states as Gaussian superpositions of yrast eigenstates centered around P_0 with width ΔP:

$$|P_0\rangle = \sum_q C_q^{P_0} |q, \mathrm{yr}\rangle, \tag{3}$$

$$C_q^{P_0} = A e^{-\frac{(q-P_0)^2}{4\Delta P^2} + i\frac{qX_0}{\hbar}}, \tag{4}$$

where X_0 is a displacement. The time evolution is given by $|P_0(t)\rangle = \exp(-i\hat{H}t/\hbar)|P_0\rangle$. As the main observable, we construct the single-particle density $n(x,t) = \langle P_0(t)|\hat{\rho}(x)|P_0(t)\rangle$ as

$$n(x,t) = \sum_{p,q} C_q^{P_0 *} C_p^{P_0} \langle q, \mathrm{yr}|\hat{\rho}(0)|p, \mathrm{yr}\rangle \times \exp[i(p-q)x/\hbar - i(E_p - E_q)t/\hbar], \tag{5}$$

where the density form factor $\langle q, \mathrm{yr}|\hat{\rho}(0)|p, \mathrm{yr}\rangle$ is calculated from the rapidities $\{k_j\}$ using formulas derived from the algebraic Bethe ansatz [23, 37–40]. Density profiles of equal-weight superpositions over all yrast states were previously shown to produce localised but rapidly dispersing depressions translating at different velocities from those of fitted GP dark soliton profiles [23, 24].

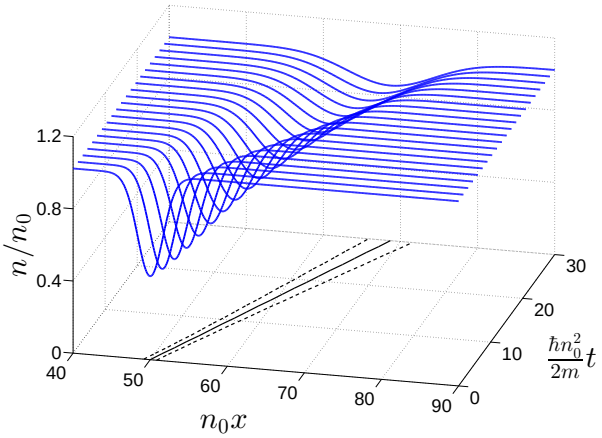

FIG. 1. Time evolution of the quantum dark soliton (3) constructed as a superposition of yrast eigenstates of the Lieb-Liniger model with $N = 100$ particles at the intermediate interaction strength $\gamma = 1$, where $\gamma = c/n_0$ and $n_0 = N/L$. The superposition is prepared with $\Delta P = 0.11\pi\hbar n_0$ and $P_0 = 0.64\pi\hbar n_0$. The solid line tracks the minimum of the dip and the dashed lines on either side of it are displaced by half of the soliton's width, i.e. by $\pm\Delta X/2$ [see Eq. (6)].

Figure 1 shows the time evolution of the density profile with initial state (3). Numerical simulations with varying parameters consistently show a smooth and localised density dip that propagates at constant velocity v_s with $X(t) = X_0 - v_\mathrm{s}t$ while the width ΔX increases over time. Here, $X \equiv \overline{x}$ measures the position, and the variance

$$\Delta X^2 = \overline{x^2} - \overline{x}^2 \tag{6}$$

the width. The average $\overline{A} = \int A\tilde{n}\, dx/N_\mathrm{d}$ is evaluated with respect to the density deviation $\tilde{n} = n(x) - n_\mathrm{bg}$ from the constant background n_bg, where $N_\mathrm{d} = \int \tilde{n}\, dx$ is the particle number depletion. In our time-dependent simulations, N_d remains approximately constant over time. Motion at constant velocity and N_d with expanding width (i.e. "greying of the dark soliton") are exactly as expected for quantum dark solitons [11, 13, 14, 41, 42].

IV. THEORY OF QUANTUM DARK SOLITONS

We aim to formulate a quantitative theory of the observed propagation at constant velocity v_s and the spreading of the soliton width. In analogy to the case of bright quantum solitons [29, 30], which consist of finite-size bound states of bosons with a quantum mechanical center-of-mass motion, we assume that the variance of the solitonic dip in the single-particle density of a Gaussian superposition state, ΔX^2, can be decomposed as

$$\Delta X^2(t) = {\sigma_\mathrm{fs}}^2 + \sigma_\mathrm{CoM}^2(t), \tag{7}$$

where ${\sigma_\mathrm{fs}}^2$ is the variance of the fundamental soliton, which is constant in time and independent of the superposition parameters ΔP and X_0 [43]. The center-of-mass variance $\sigma_\mathrm{CoM}^2(t)$ follows the time evolution of a Gaussian wave-packet in the single-particle Schrödinger equation, given by

$$\sigma_\mathrm{CoM}^2(t) = \sigma_0^2 \left[1 + \left(\frac{\hbar t}{2M\sigma_0^2}\right)^2\right], \tag{8}$$

where

$$\sigma_0^2 = \frac{\hbar^2}{4\Delta P^2} \tag{9}$$

is the initial variance of the Gaussian wave-packet density in real space and M is a mass parameter. The quadratic-in-time growth of the variance is characteristic of ballistic motion and is faster than diffusion [44]. The same effect is expected for bright solitons [29–31].

The three constant parameters – the soliton velocity v_s, fundamental width σ_fs, and mass M – completely characterise the motion of the first and second moment of the quantum dark soliton according to Eqs. (7) – (9). We have performed extensive quantum simulations of the density profile with Eq. (5) and found excellent agreement with this model for a wide range of parameters, as shown in Fig. 2 (as long as $L \gg \Delta X$ and $\Delta P \ll \pi\hbar n_0$). Interpreting quantum dark solitons as

quasi-particles in Landau's sense [32], it is not surprising that the soliton velocity observed in simulations agrees with the group velocity dE/dP and the mass parameter M with the inertial mass $(d^2E/dP^2)^{-1}$ of the yrast dispersion relation.

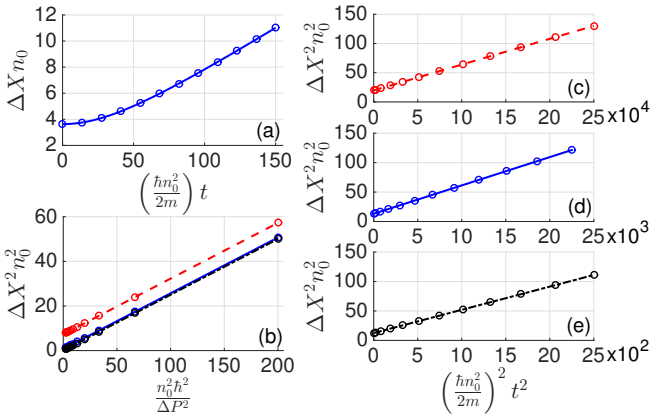

FIG. 2. Width ΔX of the density depression from simulations (symbols) compared with fits of Eq. (7) (lines). (a) Ballistic growth of ΔX in time for $\gamma = 1$ with $\sigma_{\rm fs}$ and M fitted. (b) Initial variance ΔX^2 at $t = 0$ vs. ΔP^{-2} used for extracting ${\sigma_{\rm fs}}^2$ as the intercept. Interaction strengths $\gamma = 0.1, 1, 10$ are shown by red dashed, blue continuous and black dotted lines, respectively. Panels (c), (d), (e) show linear fits of ΔX^2 vs. t^2 used to extract M for $\gamma = 0.1, 1, 10$, respectively, with $\Delta P = 0.045\pi\hbar n_0$. All panels used $P_0 = \pi\hbar n_0$ and $N = 100$. The expected quadratic dependence of the variance on $1/\Delta P$ and t is evident in all parameter regimes.

V. YRAST DISPERSION RELATION

The yrast excitation energy $E_P^N - E_0^N$ becomes a continuous function $E_{\rm s}^\infty(P)$ of momentum in the thermodynamic limit where $N, L \to \infty$ while $n_0 = N/L$ remains constant. The continuous dispersion relation can be obtained by solving Fredholm integral equations [34] and is useful for obtaining various relevant properties for the quasiparticle description as derivatives, e.g. the quasiparticle velocity $v_{\rm s} = dE_{\rm s}^\infty/dP$ and inertial mass $m_{\rm I}^{-1} = d^2E_{\rm s}^\infty/dP^2$, pertaining to an infinite system. In order to obtain quantitative agreement with our numerical simulations, finite-size corrections need to be applied. The leading $1/L$ correction terms is found from a conceptually-simple argument assuming that yrast states are associated with (soliton-like) quasiparticles with two features, in particular: (a) A particle number depletion $N_{\rm d}$ arising from a density dip that is localised on a scale that is small compared to the box size L, which leads to an elevated background density $n_{\rm bg} = n_0 - N_{\rm d}/L > n_0$, and (b) a nominal "phase step" $\Delta\phi$ that leads to a backflow current with velocity $v_{\rm cf} = \hbar\Delta\phi/mL$. This background current corresponds to a linear phase gradient that connects the phase step at the soliton across the periodic boundary conditions. The soliton moving on the background experiences a Galilean boost. The finite system dispersion relation to leading order $\mathcal{O}(L^{-1})$ is then obtained from

$$E_P^N - E_0^N \approx E_{\rm s}^N(P) \equiv E_{\rm s}^\infty(P) + P_s v_{\rm cf} + \frac{1}{2}Nmv_{\rm cf}^2 - \frac{N_{\rm d}^2}{2L}\frac{d\mu}{dn_0}, \qquad (10)$$

where $P_s = N_{\rm d} m v_{\rm s}$ is the physical momentum of the moving density depletion and the last term is a correction of the ground state energy due to the localised particle depletion obtained from a Taylor expansion of the equation of state. All quantities on the right hand side of Eq. (10) are evaluated in the thermodynamic limit at the background density $n_{\rm bg}$.

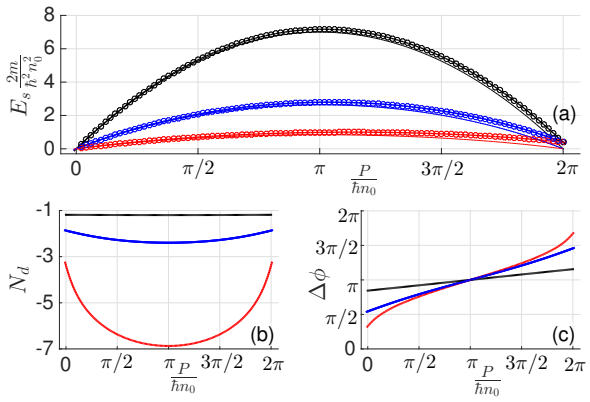

FIG. 3. (a) Dispersion relation of yrast states of the Lieb-Liniger model. Symbols show the excitation energies $E_P^N - E_0^N$ for $N = 100$ vs. momentum. Thick lines show the approximate formulae for the finite system (10) and thin lines show the dispersion relations $E_{\rm s}^\infty(P)$ in the thermodynamic limit [34] for comparison. The interaction strengths are $\gamma = 0.1$ (dashed red line & red circles), $\gamma = 1$ (full blue line & blue circles), and $\gamma = 10$ (dash-dotted black line & black circles); the same colour code is used in the bottom panels. Bottom panels: particle number depletion (c) and phase step (d) with finite size corrections for $N = 100$.

The Galilean boost demands that $P = P_{\rm s} + Nmv_{\rm cf}$, which can be used to determine the backflow velocity $v_{\rm cf}$, and hence the phase step $\Delta\phi$, once the particle number depletion $N_{\rm d}$ is known. The latter can be computed from the dispersion relation as [45, 46]

$$N_{\rm d} = -\left(1 - \frac{v_{\rm s}^2}{v_{\rm c}^2}\right)^{-1}\left(\frac{\partial E_{\rm s}^\infty}{\partial\mu} + \frac{v_{\rm s}P}{mv_{\rm c}^2}\right), \qquad (11)$$

where the derivative has to be taken at constant P and c, $v_{\rm c}$ is the speed of sound defined by $mv_{\rm c}^2 = n_0\, d\mu/dn_0$, and $\mu = \lim_{N\to\infty} dE_0^N/dN$ is the chemical potential of the ground state. Equation (11) was derived under similar assumptions to (a) and (b). For GP dark solitons in an infinite box the assumptions hold and Eq. (11) becomes exact. The dispersion relation is show in Fig. 3 (a). Both $N_{\rm d}$ and $\Delta\phi$ are shown in the bottom panels of Fig. 3. Finite size corrections to these quantities simply amount to solving the thermodynamic limit Bethe ansatz equations and evaluating $N_{\rm d}$ and $\Delta\phi$ at the elevated background density $n_{\rm bg}$.

Even though the assumptions of a localised density dip (a) and a phase step responsible for a superfluid current (b)

are not obviously satisfied for type-II Lieb-Liniger states, we find that, as for GP dark solitons, the continuous approximation of the dispersion relation is excellent in all interaction regimes as long as $\sigma_{\rm fs} \ll L$ [47] (see Fig. 3). In the Tonks-Girardeau limit of $\gamma \to \infty$ the approximation (10) becomes exact with $N_{\rm d} = -1$, $\Delta\phi = \pi$ and $E_{\rm s}^N(P) = [-P^2 + 2Pp_{\rm F}(1 + N^{-1})]/2m$, where $p_{\rm F} = \pi n_0 \hbar$ is the Fermi momentum. This approximation works very well in all regimes, which implies that the concepts of a phase step and global backflow current are useful despite the fact that global phase coherence is not expected due to strong fluctuations in 1D leading to algebraic off-diagonal long-range order.

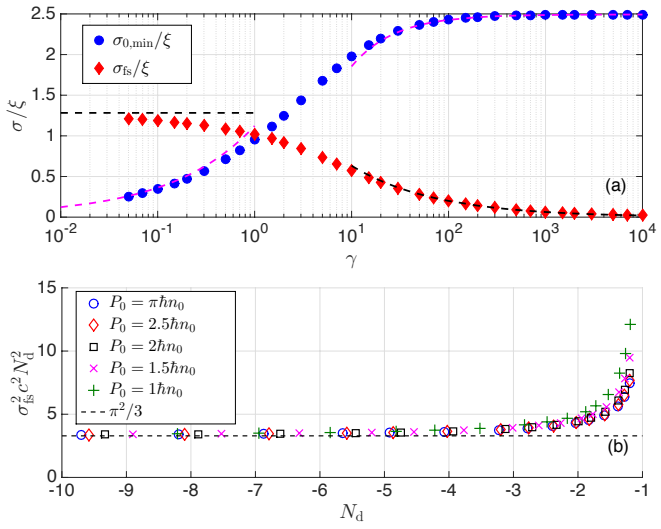

FIG. 4. Length scales of the quantum dark soliton. (a) Fundamental soliton width $\sigma_{\rm fs}$ and minimum center-of-mass wave-packet width $\sigma_{0,\rm min} \approx 0.8 n_0^{-1}$ vs. coupling strength $\gamma = c/n_0$ for $P_0 = \pi\hbar n_0$. Limiting analytical approximations: $\sigma_{\rm fs}/\xi \to \pi/\sqrt{6}$ from GP theory for $\gamma \ll 1$ and Eq. (12) for $\gamma \gg 1$ (black dashed lines). Magenta dashed lines: $\sigma_{0,\rm min}/\xi$ with $\xi \sim 1/(n_0\sqrt{2\gamma})$ for $\gamma \ll 1$ and $\xi \sim n_0^{-1}\pi^{-1}(1 + 8/3\gamma)$ for $\gamma \gg 1$. (b) Numerical data for ${\sigma_{\rm fs}}^2$ (multiplied by $c^2 N_{\rm d}^2$) vs. the particle number depletion $N_{\rm d}$ from Eq. (11) (with finite size corrections). Data from different momenta and coupling strengths collapse onto the same curve and deviate from the result $\sigma_{\rm GP}^2$ (dashed line) for the classical dark soliton only near the Tonks-Girardeau limit where $N_{\rm d} \to -1$. The width $\sigma_{\rm fs}$ was extracted from simulation data with $N = 100$.

VI. LENGTH SCALES

In contrast to a classical soliton, which propagates with constant shape, the density profile of the quantum dark soliton changes in time. According to Eqs. (7) & (8) the strongest localization occurs at $t = 0$ and is determined by the fundamental soliton width $\sigma_{\rm fs}$ together with the length scale of the Gaussian wave packet σ_0. The choice of the latter is limited by the requirement of ΔP fitting in to the fundamental momentum interval $[0, 2\pi\hbar n_0]$. We estimate the minimal value $\sigma_{0,\rm min}$ conservatively from Eq. (9) with $\Delta P \lesssim \pi\hbar n_0/5$. Figure 4 (a) shows the two length scales $\sigma_{\rm fs}$ and $\sigma_{0,\rm min}$ crossing over at intermediate interactions, with the size of the quantum dark soliton limited by the larger length scale.

The fundamental soliton width $\sigma_{\rm fs}$ is an interesting nontrivial quantity that we extract from numerical simulations by fitting [see Fig. 2 (b)]. For small γ our data agree very well with the dark soliton width computed from the GP equation according to Eq. (6), $\sigma_{\rm GP} = \pi\xi/\sqrt{6(1 - v_{\rm s}^2/v_{\rm c}^2)}$, where $\xi = \hbar/\sqrt{2m\mu}$, while for large γ the fundamental soliton width $\sigma_{\rm fs}/\xi$ tends to zero. Close inspection reveals that

$$\sigma_{\rm fs}/\xi \approx 2/\sqrt{\gamma} \quad \text{for} \quad \gamma \gg 1 \tag{12}$$

fits the numerical data very well [see Fig. 4 (a)]. The vanishing of $\sigma_{\rm fs}$ demonstrates that the fundamental soliton changes from a macroscopic object in the Bogoliubov regime, where it coincides with the GP dark soliton, to a single-particle hole without an intrinsic length scale in the Tonks-Girardeau limit.

It is tempting to interpret the quantum dark soliton as a bound state of $|N_{\rm d}|$ holes (a fractional number) in analogy to quantum bright solitons, which are bound states of N bosons [29], where the fundamental soliton width is a length scale of the multi-particle bound state [30]. Indeed, the length scale $\sigma_{\rm GP}$ for the GP dark soliton can be re-expressed as $\sigma_{\rm GP} = \pi/(\sqrt{3}c|N_{\rm d}^{\rm GP}|)$, where the velocity-dependence is fully subsumed in the particle number depletion $N_{\rm d}^{\rm GP}$. Plotting numerical data for $\sigma_{\rm fs}$ vs. $N_{\rm d}$ in Fig. 4 demonstrates that data taken at different interaction strengths $\gamma = c/n_0$ and momenta P_0 falls onto a single curve within numerical accuracy, which means that $\sigma_{\rm fs}$ also appears to depend directly only on $N_{\rm d}$ and c. Significant deviations from the GP formula are observed only close to $N_{\rm d} = -1$, which corresponds to the strongly correlated Tonks-Girardeau limit.

Interpreting the quantum soliton as a bound state of holes with quantum-mechanical center-of-mass motion is consistent with lattice simulations at small γ [15]. These showed that imprinted dark solitons display an innate soliton profile with constant length scale in single-shot images, while the single-particle density displays a spreading and weakening depression over time due to a growing uncertainty over the soliton position. Our results quantify these effects and suggest that the same physical picture is relevant far into the strongly correlated regime.

Classical solitons emerge in our theory in the Bogoliubov limit $\gamma \to 0$, where $\sigma_{\rm fs} \to \pi\xi/\sqrt{6} = \pi/\sqrt{12\gamma}n_0$ and $M \to 2mN_{\rm d} \to -4m\sqrt{1 - v_{\rm s}^2/v_{\rm c}^2}/\sqrt{\gamma}$ become macroscopic. Constructing a wave packet with $\epsilon \equiv \Delta P/2\pi n_0\hbar \ll 1$, we find that the initial soliton can be well localised ($\sigma_0 \ll \sigma_{\rm fs}$) when $\epsilon^2 \gg 3\gamma/4\pi^4$ and remains so (${\sigma_{\rm CoM}^2 - \sigma_0^2} \ll {\sigma_{\rm fs}}^2$) for a time $t \ll \sqrt{1 - v_{\rm s}^2/v_{\rm c}^2}m/(\sqrt{6}\gamma\epsilon\hbar n_0^2)$. We have further verified that numerical density profiles at $\gamma = 0.01$ are nearly indistinguishable from GP solitons at the same momentum P_0.

VII. CONCLUSIONS

The yrast states of the Lieb-Liniger model are strongly correlated, fragmented [19, 48], and contain relevant information about the solitonic dip in high order correlation functions

[22]. In this situation it may seem remarkable and surprising that solitonic physics can be extracted from the single-particle density of superposition states and easily quantified by the hypothesized equations (7) – (9). On the other hand it is known from the theory of quantum bright solitons, that wave-packet superpositions of fragmented and translationally invariant eigenstates can achieve almost unit condensate fraction [31]. Such states are only weakly correlated and closely resemble bright solitons of typical ultra-cold gas experiments (e.g. Ref. [49]). While our computational approach does not provide access to the condensate fraction, there is nevertheless good reason to believe that the initial superposition states of our simulations [Eq. (3)] for small γ are weakly correlated as well and closely resemble the quantum states prepared in dark soliton experiments with Bose-Einstein condensates, e.g. in Refs. [3, 5, 6]. A suitable preparation protocol for quantum dark solitons is thus to prepare a dark soliton in the small γ regime, e.g. by standard phase imprinting [2, 3], possibly enhanced by density engineering [50], and then ramp the coupling strength γ to the desired value by means of a Feshbach or confinement-induced resonance [51].

We have prepared the candidate quantum dark soliton of Eq. (3) as a Gaussian superposition of yrast states, and the properties of Gaussian wave packets have led us to hypothesise the equations for the width of the density feature (7) – (9). Given that these equations are well supported by numerical evidence, we may hope that they can eventually be proven within the framework of the Bethe ansatz, and validated by experiments. While the Gaussian profile of Eq. (4) was a somewhat arbitrary choice, it seems reasonable to expect that Eqs. (7) – (9) are only true for Gaussian profiles, and that an uncertainty relation of the form

$$\Delta P \sqrt{\Delta X^2 - {\sigma_{\rm fs}}^2} \leq \frac{\hbar}{2}, \tag{13}$$

holds for arbitrary superpositions in analogy to the well-known position–momentum uncertainty for point particles. In this more general context, ΔX and ΔP represent measurable quantities while $\sigma_{\rm fs}$ is an intrinsic property of the dominant yrast state. The Gaussian profile at $t = 0$ then realises equality in the relation (13) as a minimum uncertainty wave packet. The Gaussian superposition thus presents an "optimal quantum dark soliton" by obeying Eqs. (7) – (9). The properties of quantum states constructed using Bogoliubov theory in Ref. [11] correspond to optimal quantum dark solitons in this sense, while the equal-weight superposition of all yrast states in the interval $q \in [0, 2\pi n_0 \hbar)$ of Ref. [24] falls outside of this framework.

The significance of the results presented here goes beyond the specific exactly-solvable model. The emerging picture of quasiparticle dynamics of yrast excitations in a strongly correlated quantum fluid is so simple and intuitive that we may expect it to be valid for non-integrable systems as well, e.g. ultracold atoms with dipolar interactions, electrons in quantum wires, or Josephson vortices in coupled Bose gases [52]. By simple extension, our framework allows for the study of soliton collisions, the results of which are left for a future publication.

ACKNOWLEDGMENTS

We thank G. Astrakharchik for discussion. JB thanks the Max Planck Institute for Solid State Research for hospitality during a stay where part of this work was completed. This work was partially supported by the Marsden fund of New Zealand (contract number MAU1604) and by a grant from the Simmons Foundation. This work was performed in part at Aspen Center for Physics, which is supported by National Science Foundation grant PHY-1607611. SS was supported by the Massey University Doctoral Research Dissemination Grant.

[1] Toshio Tsuzuki, "Nonlinear waves in the Pitaevskii-Gross equation," J. Low Temp. Phys. **4**, 441 (1971).

[2] J. Denschlag, J. E. Simsarian, D. L. Feder, Charles W. Clark, L. A. Collins, J. Cubizolles, L. Deng, E. W. Hagley, K. Helmerson, William P. Reinhardt, S. L. Rolston, B. I. Schneider, and William D. Phillips, "Generating Solitons by Phase Engineering of a Bose-Einstein Condensate," Science **287**, 97–101 (2000).

[3] S. Burger, K. Bongs, S. Dettmer, W. Ertmer, K. Sengstock, A. Sanpera, G. V. Shlyapnikov, and M. Lewenstein, "Dark Solitons in Bose-Einstein Condensates," Phys. Rev. Lett. **83**, 5198–5201 (1999).

[4] Naomi S. Ginsberg, Joachim Brand, and Lene Vestergaard Hau, "Observation of Hybrid Soliton Vortex-Ring Structures in Bose-Einstein Condensates," Phys. Rev. Lett. **94**, 040403 (2005), arXiv:0408464 [cond-mat].

[5] Christoph Becker, Simon Stellmer, Parvis Soltan-Panahi, Sören Dörscher, Mathis Baumert, Eva-Maria Richter, Jochen Kronjäger, Kai Bongs, and Klaus Sengstock, "Oscillations and interactions of dark and dark-bright solitons in Bose-Einstein condensates," Nat. Phys. **4**, 496–501 (2008).

[6] A. Weller, J. P. Ronzheimer, C. Gross, J. Esteve, M. K. Oberthaler, D. J. Frantzeskakis, G. Theocharis, and P. G. Kevrekidis, "Experimental observation of oscillating and interacting matter wave dark solitons," Phys. Rev. Lett. **101**, 130401 (2008), arXiv:0803.4352.

[7] Giacomo Lamporesi, Simone Donadello, Simone Serafini, Franco Dalfovo, and Gabriele Ferrari, "Spontaneous creation of KibbleZurek solitons in a BoseEinstein condensate," Nat. Phys. **9**, 656–660 (2013), arXiv:1306.4523.

[8] Mark J. H. Ku, Biswaroop Mukherjee, Tarik Yefsah, and Martin W Zwierlein, "Cascade of Solitonic Excitations in a Superfluid Fermi gas: From Planar Solitons to Vortex Rings and Lines," Phys. Rev. Lett. **116**, 045304 (2016), arXiv:1507.01047.

[9] Tarik Yefsah, Ariel T Sommer, Mark J H Ku, Lawrence W. Cheuk, Wenjie Ji, Waseem S Bakr, and Martin W Zwierlein, "Heavy solitons in a fermionic superfluid." Nature **499**, 426–30 (2013), arXiv:1302.4736.

[10] G. E. Astrakharchik and L. P. Pitaevskii, "Lieb's soliton-like excitations in harmonic trap," EPL (Europhysics Lett. **102**, 30004 (2012), arXiv:1210.8337.

[11] J. Dziarmaga, "Quantum dark soliton: Nonperturbative diffusion of phase and position," Phys. Rev. A **70**, 063616 (2004).

[12] R. V. Mishmash and L. D. Carr, "Quantum Entangled Dark Solitons Formed by Ultracold Atoms in Optical Lattices," Phys. Rev. Lett. **103**, 140403 (2009).

[13] Jacek Dziarmaga, Zbyszek P Karkuszewski, and Krzysztof Sacha, "Quantum depletion of an excited condensate," Phys. Rev. A **66**, 043615 (2002), arXiv:0110080 [cond-mat].

[14] Jacek Dziarmaga and Krzysztof Sacha, "Depletion of the dark soliton: The anomalous mode of the Bogoliubov theory," Phys. Rev. A **66**, 043620 (2002).

[15] Dominique Delande and Krzysztof Sacha, "Many-Body Matter-Wave Dark Soliton," Phys. Rev. Lett. **112**, 040402 (2014).

[16] P. P. Kulish, S. V. Manakov, and L. D. Faddeev, "Comparison of the exact quantum and quasiclassical results for a nonlinear Schrödinger equation," Theor. Math. Phys. **28**, 615–620 (1976).

[17] Masakatsu Ishikawa and Hajime Takayama, "Solitons in a One-Dimensional Bose System with the Repulsive Delta-Function Interaction," J. Phys. Soc. Japan **49**, 1242–1246 (1980).

[18] R. Kanamoto, L. D. Carr, and M. Ueda, "Metastable quantum phase transitions in a periodic one-dimensional Bose gas. II. Many-body theory," Phys. Rev. A **81**, 023625 (2010), arXiv:0910.2805.

[19] Oleksandr Fialko, Marie-Coralie Delattre, Joachim Brand, and Andrey Kolovsky, "Nucleation in Finite Topological Systems During Continuous Metastable Quantum Phase Transitions," Phys. Rev. Lett. **108**, 250402 (2012), arXiv:1202.5083.

[20] A Roussou, J Smyrnakis, M Magiropoulos, Nikolaos K Efremidis, and G M Kavoulakis, "Rotating Bose-Einstein condensates with a finite number of atoms confined in a ring potential: Spontaneous symmetry breaking beyond the mean-field approximation," Phys. Rev. A **95**, 033606 (2017).

[21] A. D. Jackson, J. Smyrnakis, M. Magiropoulos, and G. M. Kavoulakis, "Solitary waves and yrast states in Bose-Einstein condensed gases of atoms," EPL (Europhysics Lett. **95**, 30002 (2011).

[22] Andrzej Syrwid and Krzysztof Sacha, "Lieb-Liniger model: Emergence of dark solitons in the course of measurements of particle positions," Phys. Rev. A **92**, 032110 (2015), arXiv:1505.06586.

[23] Jun Sato, Rina Kanamoto, Eriko Kaminishi, and Tetsuo Deguchi, "Exact relaxation dynamics of a localized many-body state in the 1D Bose gas," Phys. Rev. Lett. **108**, 110401 (2012), arXiv:1112.4244.

[24] Jun Sato, Rina Kanamoto, Eriko Kaminishi, and Tetsuo Deguchi, "Quantum states of dark solitons in the 1D Bose gas," New J. Phys. **18**, 075008 (2016), arXiv:1602.08329.

[25] Andrzej Syrwid, Mirosław Brewczyk, Mariusz Gajda, and Krzysztof Sacha, "Single-shot simulations of dynamics of quantum dark solitons," Phys. Rev. A **94**, 023623 (2016), arXiv:1605.08211.

[26] M. Rosenbluh and R. M. Shelby, "Squeezed optical solitons," Phys. Rev. Lett. **66**, 153–156 (1991).

[27] P. D. Drummond, R. M. Shelby, S. R. Friberg, and Y Yamamoto, "Quantum solitons in optical fibres," Nature **365**, 307–313 (1993).

[28] J. B. McGuire, "Study of Exactly Soluble One-Dimensional N-Body Problems," J. Math. Phys. **5**, 622–636 (1964).

[29] Y Lai and HA Haus, "Quantum theory of solitons in optical fibers. II. Exact solution," Phys. Rev. A **40**, 854–866 (1989).

[30] Jayson G. Cosme, Christoph Weiss, and Joachim Brand, "Center-of-mass motion as a sensitive convergence test for variational multimode quantum dynamics," Phys. Rev. A **94**, 043603 (2016), arXiv:1510.07845.

[31] Alex Ayet and Joachim Brand, "The single-particle density matrix of a quantum bright soliton from the coordinate Bethe ansatz," J. Stat. Mech. Theory Exp. **2017**, 023103 (2017), arXiv:1510.04311.

[32] Vladimir V. Konotop and Lev Pitaevskii, "Landau Dynamics of a Grey Soliton in a Trapped Condensate," Phys. Rev. Lett. **93**, 240403 (2004).

[33] Elliott H. Lieb and Werner Liniger, "Exact Analysis of an Interacting Bose Gas. I. The General Solution and the Ground State," Phys. Rev. **130**, 1605–1616 (1963).

[34] Elliott H. Lieb, "Exact Analysis of an Interacting Bose Gas. II. The Excitation Spectrum," Phys. Rev. **130**, 1616–1624 (1963).

[35] Note that $c = -2/a_{1D} = gm/\hbar^2$, where a_{1D} is the 1D scattering length and g the effective coupling constant [53].

[36] C. N. Yang and C. P. Yang, "Thermodynamics of a OneDimensional System of Bosons with Repulsive DeltaFunction Interaction," J. Math. Phys. **10**, 1115–1122 (1969).

[37] N. A. Slavnov, "Calculation of scalar products of wave functions and form factors in the framework of the algebraic Bethe ansatz," Theor. Math. Phys. **79**, 502–508 (1989).

[38] N. A. Slavnov, "Nonequal-time current correlation function in a one-dimensional Bose gas," Theor. Math. Phys. **82**, 273–282 (1990).

[39] V. E. Korepin, "Calculation of norms of Bethe wave functions," Commun. Math. Phys. **86**, 391–418 (1982).

[40] Jean-Sébastien Caux, Pasquale Calabrese, and Nikita A. Slavnov, "One-particle dynamical correlations in the one-dimensional Bose gas," J. Stat. Mech. Theory Exp. **2007**, P01008–P01008 (2007).

[41] C. K. Law, "Dynamic quantum depletion in phase-imprinted generation of dark solitons," Phys. Rev. A **68**, 015602 (2003).

[42] R. V. Mishmash, I. Danshita, Charles W. Clark, and L. D. Carr, "Quantum many-body dynamics of dark solitons in optical lattices," Phys. Rev. A **80**, 053612 (2009), arXiv:0906.4949.

[43] A corresponding result to Eq. (7) was proved in Ref. [30].

[44] In regular diffusion the growth of the variance is linear in time. The term "quantum diffusion" for quantum solitons that is found in the literature [11] is thus a misnomer.

[45] M. Schecter, D.M. Gangardt, and A. Kamenev, "Dynamics and Bloch oscillations of mobile impurities in one-dimensional quantum liquids," Ann. Phys. (N. Y). **327**, 639–670 (2012).

[46] Sophie S. Shamailov and Joachim Brand, "Dark-soliton-like excitations in the Yang-Gaudin gas of attractively interacting fermions," New J. Phys. **18**, 075004 (2016), arXiv:1603.04864.

[47] This condition is easily violated near the edges of the dispersion relation, i.e. $P_0 \approx 0, 2\pi\hbar n_0$, and for very weak interactions in a finite box.

[48] Rafał Ołdziejewski, Wojciech Górecki, Krzysztof Pawłowski, and Kazimierz Rzążewski, "Many-body soliton-like states of the bosonic ideal gas," (2018), arXiv:1803.11042.

[49] L Khaykovich, "Formation of a Matter-Wave Bright Soliton," Science **296**, 1290–1293 (2002).

[50] L. D. Carr, J. Brand, S. Burger, and A. Sanpera, "Dark-soliton creation in Bose-Einstein condensates," Phys. Rev. A **63**, 051601(R) (2001).

[51] E Haller, M Gustavsson, M J Mark, J G Danzl, R Hart, G Pupillo, and H.-C. Nagerl, "Realization of an Excited, Strongly Correlated Quantum Gas Phase," Science **325**, 1224–1227 (2009), arXiv:1006.0739.

[52] Sophie S. Shamailov and Joachim Brand, "Quasiparticles of

widely tuneable inertial mass: The dispersion relation of atomic Josephson vortices and related solitary waves," SciPost Phys. **4**, 018 (2018), arXiv:1709.00403.

[53] M Olshanii, "Atomic Scattering in the Presence of an External Confinement and a Gas of Impenetrable Bosons," Phys. Rev. Lett. **81**, 938–941 (1998).